RESEARCH PAPER

Simple and low-cost fabrication of PDMS microfluidic round channels by surface-wetting parameters optimization

**Magalie De Ville · Philippe Coquet ·
Philippe Brunet · Rabah Boukherroub**

Abstract Convenient for both biologists and MEMS designers, Polydimethylsiloxane (PDMS) polymer is intensively investigated for its biocompatibility, transparency, high resistance under plasma treatment, flexibility and resistance to high temperature. However, for microfluidic applications, the fabrication of PDMS circular channels is difficult to achieve except by wire moulding. In this article, we present a simple, fast and low-cost fabrication method which can be applied out of clean-room environment. It is based on the deposition of alginic acid sodium salt aqueous solution, enabling the formation of a liquid cylinder on the most hydrophilic part of a hydrophilic/hydrophobic patterned surface. We experimentally studied the interaction between liquid rivulets and surfaces presenting a contrast of wettability and/or a stepwise texture. Subsequent moulding of the half-cylinder of liquid produces round PDMS microfluidic channels. The optimal parameters for hydrophilic/hydrophobic patterns have then been applied to produce the roundest possible channels. The realisation of both straight channels 300–500 μm wide, 1 cm long and 75° tangent chord angle at best, and Y-shaped channels with the same dimensions and 55° TCA is demonstrated.

Keywords Round-channels · PDMS · Alginate · Patterning · Wetting

M. De Ville (✉) · P. Coquet · P. Brunet · R. Boukherroub
Institut d'Electronique, de Microélectronique et de
Nanotechnologie, CNRS UMR 8520, Avenue Poincaré,
59658 Villeneuve d'Ascq, France
e-mail: magalie.de-ville@ed.univ-lille1.fr

1 Introduction

Closed and perfectly circular channels are of great interest for the mimicry of biological systems like vein networks. In this optic the use of a "green" approach is also highly desirable, and the notion of a "single-use" chip is necessarily associated to the requirement of a low-cost process. The circular shape of a microchannel constitutes the optimal condition for the generation of a fixed flow-rate at minimal pressure (Mortensen et al. 2005). Indeed, the pressure required to create a flow at a given rate in a circular channel is minimal, as compared to that in a rectangular channel of similar dimensions. Therefore, the challenge is to design solid channels with a tangent chord angle (TCA) α close to 90° (Fig. 1), by exploiting materials as supports and varying their surface contact angles (SCA).

The TCA tally to the final angle of the solid channel and SCAs tally to the angle θ involved in the Young's relation for a liquid in air: $\cos\theta = (\gamma_s - \gamma_{sl})/\gamma_{lv}$, where γ_s is the surface tension of the solid surface, γ_{sl} is the solid–liquid surface tension and γ_{lv} is the liquid–vapour surface tension.

Furthermore, the versatile and exhaustive fabrication of such channels in various configurations requires processes based on simple and low-cost steps, in the spirit of what we propose in the present study. The fabrication of round channels for microfluidics has recently attracted much attention within a host of different methods described thereafter.

A first approach consists on the generation of solid moulds with a round shape. A conventional way is photolithography: Futai et al. (2004) used a backside diffused light photography strategy combined with small aperture sizes on their photomask to produce 200 μm wide semiround channels. Wang et al. (2007) have fabricated 500 μm wide and 70° TCA channels using a negative photoresist
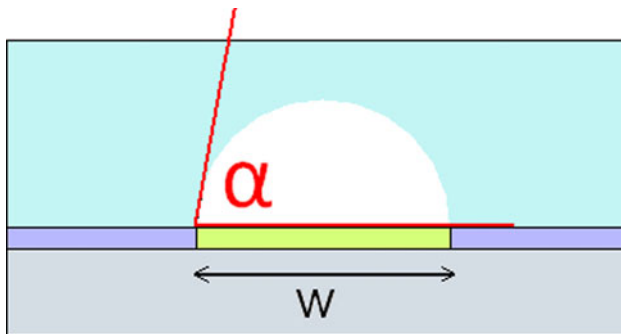
Fig. 1 Sketch of the cross section of a channel. α is the tangent chord angle of the channel, *W* denotes the width of the inner hydrophilic green domain (SCA 1) compared to the outer hydrophobic *purple* domain (SCA 2) of the *grey* supporting material. We have of course SCA 1 < SCA 2. The *light blue colour* corresponds to the final solid channel

(THB 120N from JSR Inc.) with a reflow after development. A positive photoresist (AZ9260, Hoechst) combined to a plasma polymerization technique of tetramethyldisiloxane (TMDS) was employed to create 25 μm wide straight rounded channels (Abbas et al. 2009). Channels of 180 μm width and 5° TCA were successfully obtained by photocopying patterns on a transparency (Tan et al. 2001). The dried ink was used as master to cast the PDMS, which was peeled after curing. A similar method was employed by Grimes et al. (2008). They used a shrinky-dink material which was printed with a LaserJet printer. This material is a retractable plastic sheet, enabling the shrinkage of the ink patterns by baking. Using the pattern of baked ink as master, they obtained 20° TCA for 200 μm wide channels. Independently, straight channels of 400 μm in width and 45° TCA were created by laser patterning onto PMMA (Luo et al. 2007). Channels are formed on PMMA then PDMS is poured to create the counter mould, which can be used several times to create semi-rounded channels. On the other hand, Song et al. (2010) used metal wire moulding technique to form 300 μm wide and perfectly round channels, but without any intersections. The metal was removed by heating.

Another approach is to use the viscous property of liquid PDMS before curing to achieve a coating. By stacking three layers of PDMS, keeping the interlayer in the liquid state, and the upper layer with a 300 μm wide squared channel, a meniscus was formed and gave rise to a semi-rounded channel (Lee et al. 2007). Abdelgawad et al. (2010) used straight-squared channels of PDMS, filled with liquid PDMS and they injected an air stream to produce 100 μm wide round channels with a maximum length of 16 cm. The round-shaped deformation of the PDMS membrane obtained under pressure was used to prepare 400 μm wide straight channels and 200 μm wide Y-shaped channels with 43° and 23° TCA, respectively (Hongbin

et al. 2009). Using the similar membrane technique, Kang et al. (2010) elaborated SU8 moulds and achieved channels of TCA larger than 70°, but with a width larger than 600 μm. Other strategies rely on the local modification of the surface wetting properties, on which a half-cylindrical rivulet of liquid eventually utilized as a mould can be formed, tailored and maintained. Typically, a 3D profile or a 2D stripe zone with higher surface energy, on the substrate, can help to prevent the pinch-off or the formation of bulges on such rivulets that would occur otherwise as the consequence of a capillary-originating instability (Lenz 1999; Brinkmann and Lipowsky 2002; Brinkmann and Blossey 2004; Speth and Lauga 2009). For example, West et al. (2007) used microplasma patterning of glass surfaces modified with dichlorodimethylsiloxane giving rise to flat aqueous liquid straight or Y-shaped patterns. In the same way, local degradation of PDMS by O_2 exposure using microscale plasma activated templating technique (μPLAT) provided 900 μm wide channels with 15° TCA after PDMS curing (Chao et al. 2007). Liu et al. (2009) prepared surfaces carrying out hydrogel patterns by UV lithography. Glycerol deposition is then made as liquid mould and PDMS is poured over it and cured. By this way, they have reached 20° TCA for 200 μm wide channel and 40° TCA for 400 μm wide channels for serpentine and Y shapes. Finally, some groups tried to directly etch PDMS, but this material is robust against chemical etching (Garra et al. 2002).

From these results, it is obvious that the preparation of PDMS round channels is a real challenge. The reported methods require sometimes sophisticated equipment and several steps. In the present work, we propose a simple and low-cost method to produce PDMS round channels, combining together previously reported techniques, but also differing from them by limiting both the number of time-consuming steps and the use of multi-specific equipments. Our method can be used in any lab without the need for clean-room facilities. It is based on the optimization of the wetting parameters to produce hydrophobic/hydrophilic steps for the channel pattern definition together with the use of alginic acid sodium salt aqueous solution. The specific properties of the alginic acid solution are an asset for damping interfacial instabilities and for producing the master for PDMS moulding.

Using this method we have realized two types of samples. In the first one, the channel pattern is defined as a three-dimensional (3D) structuration with stepwise variations of SCA, while in the second one, octadecyltrichlorosilane (OTS)-coated surfaces are degraded by UV in order to achieve a bi-dimensional pattern of stepwise-varying SCA. The choice between those two processes is done according to the final shape desired for the channels.

2 Materials and methods

2.1 Reagents and instruments

PDMS was purchased as Sylgard 184 from Dow Corning and prepared at classical ratio 10:1 (base:curing agent).

Isopropanol, methanol, acetone, alginic acid sodium salt A0682 powder and OTS (octadecyltrichlorosilane, 95%) were supplied from Sigma-Aldrich. One side polished *n*-type Si(100) (5–10 Ω cm^{-1}) wafers provided by Siltronix were used as substrates.

Oxford Plasmalab 80+ was used for a very clean and precise deposition of 100 nm thick CHF$_3$ layers. The following conditions were used: exposure time 25 min, power 250 W, pressure 40 mT, gas flow 30 sccm. The use of this equipment is not necessarily required, as a simple "Teflon spray" gives also quite good results.

UVO cleaner 42 (500 W mercury lamp, 253 nm UV radiation, Jelight Company Inc., USA) was used for OTS layer degradation. After 5 min irradiation, the SCA decreased from 105° to 80°.

Glovebox (PLAS-LABS type) was used for the thorough deposition of octadecyltrichlorosilane (OTS) in nitrogen atmosphere.

GBX Digidrop with CCD camera and image analysis software (ImageJ) allow the visualization of the wetting properties of the different materials by SCA measurements.

Syringes with 30G needles enable alginic acid sodium salt solution deposition.

2.2 Experimental methods

In this section, we present the two processes we developed to render possible the fabrication of round channels networks with a minimum of easily accessible equipments, a minimum of time and limited steps. Our results show that this goal is possible to reach by combining the existing techniques presented in our introduction.

Our specifications were:

- To obtain the roundest mould possible with various shapes.
- To use the viscous properties of liquids.
- To locally modify the surface wetting properties combined with a 3D structuration or a 2D stripe zone on the substrate.

Thus, let us first remind the definition of wetting properties in Fig. 2:

2.2.1 First attempt: direct degradation of PDMS

In order to produce channels with a large TCA α value, the wettability contrast between the outer (θ_{outer}) and the inner
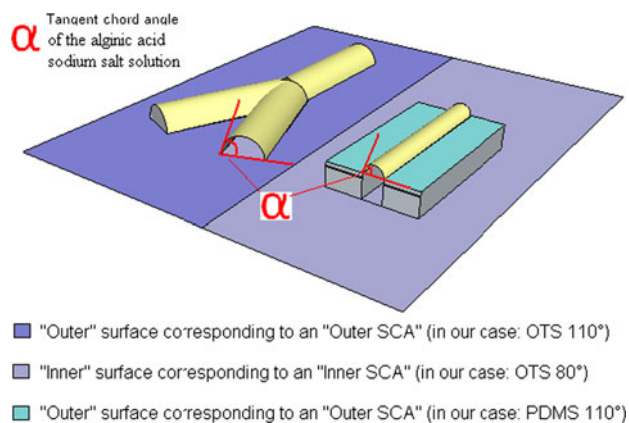

Fig. 2 Definition of the surface wetting properties

(θ_{inner}) angles was optimized. We firstly tried a method to control the surface contact angle steps by exposure of PDMS substrates to O$_2$ plasma through shadowmasks. This was mainly motivated by the simplicity of the method previously reported by Chao et al. (2007). They used microscale Plasma Activated Templating technique to create patterns on a planar PDMS surface which is locally completely degraded. There was no attempt to control the inner angle or to investigate the hydrophilic/hydrophobic contrast for the channel definition. Furthermore, their liquid mould was made of water, which led their experiments to flat channels (TCAs ~5°). In our experiments, to control the inner angle, the PDMS film was exposed to O$_2$ plasma through a shadowmask. We varied the pressure, power and time (Supporting information can be obtained from the authors) to obtain channels with TCAs from 5° to 49°. However, we have found that this method was not easily reproducible, and we have encountered similar problems of mould flattening as in Chao et al. (2007): water gives a good TCA before pouring PDMS (around 80°), and gives a final TCA of 49° (at best, as mentioned above) for the channel after demoulding, which means a decrease of 37%. Thus, we did not carry on this method further.

Our strategy has been then to work with hydrophobic surfaces; the initial coating with OTS is eventually degraded using UV/Ozone for an accurate control of both inner and outer angles.

2.2.2 How to choose the liquid for the mould?

The physical and chemical properties of the liquid serving as mould are crucial for the optimization of the quality, stability and geometrical features of the final channel.

First, a few attempts with alternative liquids were made. Water is easy to manipulate, as capillarity directs the liquid flow on the hydrophilic patterns, but the TCA of the liquid cylinder is hard to control due to fast evaporation of the

small volume involved. Moreover, the overflowing outside the patterns happens easily. In order to preserve the high TCA when the liquid PDMS is poured, gelatine and agarose aqueous solutions were also investigated. These liquids display a high density, a high viscosity, and are easily turnable from liquid to solid. However with these liquids, the main drawback is the required temperature to maintain them in the liquid state (45°C for gelatine, and 85°C for agarose), which renders difficult the deposition by syringes or capillaries.

Another reminiscent issue for liquid moulding as exposed before is the flattening during the subsequent moulding step. We have used three liquids: water, glycerol, and sodium alginate, with the properties shown in Table 1.

Our initial idea was to use a highly viscous liquid, keeping the surface tension relatively high, in order to damp the influence of external mechanical perturbations that would initiate interface instabilities. Also, glycerol and alginate are non-volatile liquids compared to water.

Assuming that the flattening could be partly due to the Rayleigh–Taylor instability (Piriz et al. 2006), the choice for the denser glycerol would be natural. This instability happens when gravity is acting on two fluids of different densities, with the denser fluid being above a fluid of lesser density. The possible consequences are that the denser liquid will replace the light one, or a mixing between the two liquids will occur. However, it turns out that the lighter sodium alginate gives the best results in terms of mould robustness against flattening.

By trying to understand this surprising result, we have noticed that a solid protective shell is formed by this liquid at the interface with PDMS, especially when the curing process is accelerated by heating at 50°C. This shell seems to resolve the evaporation problem encountered with water and it increases the crush resistance of the alginic acid sodium salt solution. Thus it permits the channel fabrication with a TCA decrease of 10° (12%) at the worst, after pouring the PDMS (Fig. 11). Therefore, the choice of sodium alginate is optimal to keep a weak flattening.

2.2.3 Ways of fabrication

Resulting from those ideas and observations, we have elaborated two fast and simple protocols for microfluidic devices fabrication.

Table 1 Liquid physical properties

Liquid	Density (g cm^{-3})	Viscosity (Pa s)	Surface tension (N m^{-1})
Glycerol	1.261	1.412	0.065
Sodium alginate	1.0072	1.642	0.075

OTS-terminated silicon surfaces used for our local modification of the surfaces wetting properties were prepared as follows: first, the wafers were oxidized during 30 min using UV/Ozone and then immersed in 5×10^{-3} M OTS/hexane solution for 4 h at room temperature. The resulting surfaces display a water SCA of 110° and a relatively low-hysteresis of about 10° to 15° (Coffinier et al. 2007).

2.2.3.1 Process I: realisation of straight channels For this first method, the patterning was achieved by cutting out rectangular stripes of PDMS coated with CHF$_3$ and by reporting them onto uniformly degraded OTS surface (SCA = 80°). These stripes are used for 3D structuration of straight channels, and are constituted of alternated layers of PDMS and CHF$_3$. They are prepared on preliminary wafers using a spin coating equipment, before their cut and their transfer, as shown in Fig. 3a. The thickness is controlled through the usual parameters: speed and time of rotation, according to Fig. 3b. The CHF$_3$ layer enables passivation and detachment of PDMS from wafers as well as layers separation.

The transfer of layers on the OTS-coated surfaces was made using a blade to cut up a straight channel in a full strip, removing the exceeding using tweezers. Figure 4 illustrates the patterning process leading to straight channels:

Our choice to create stacks of PDMS and CHF$_3$ layers is motivated by the ability to remove the effect of the height of the PDMS steps after moulding as explained later.

2.2.3.2 Process II: realisation of channels with cross-links For this second method, patterning was performed through a shadowmask to locally degrade OTS layer using UV/O$_3$ treatment. This method enables to obtain a pattern with a more complex geometry compared to process I.
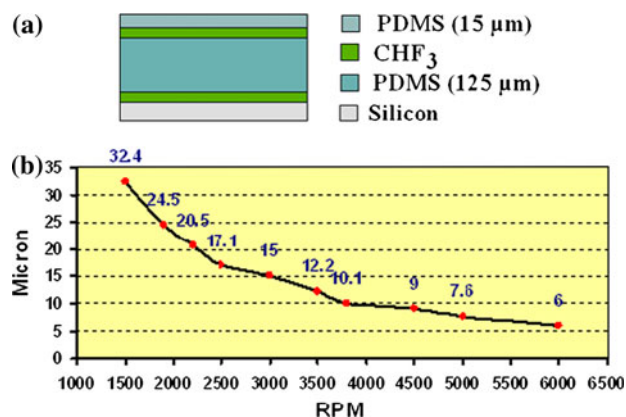

Fig. 3 a PDMS and CHF$_3$ layers, deposited on a silicon substrate, used for the process I, **b** parameters for thin PDMS layers deposition
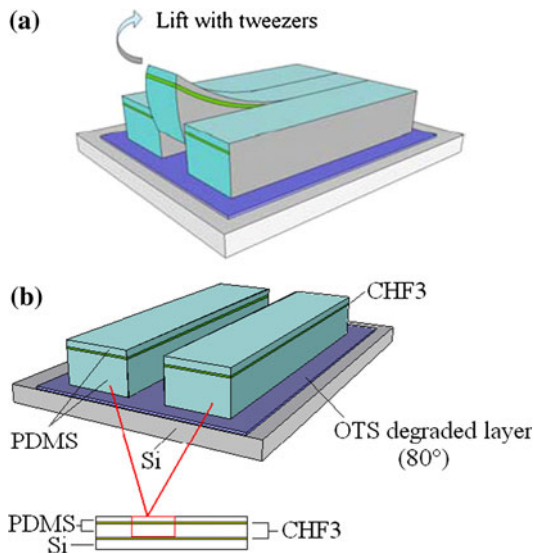
Fig. 4 Process I using layers patterning on OTS-terminated silicon substrate uniformly degraded (SCA = 80°) by (**a**) reporting PDMS/CHF₃ stacks, **b** blade cutting and lift with tweezers
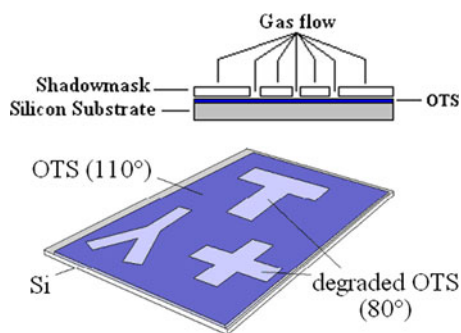

Fig. 5 Schematic illustration of OTS patterning using a shadowmask for process II

Shadowmasks were designed using clewin3 software, and used to create hydrophobic/hydrophilic contrast on the OTS-terminated surfaces as shown in Fig. 5.

For convenience we have fabricated the shadowmask using clean room facilities, but they can be produced at low cost using mechanical manufacturing.

The fabrication of the shadowmask involves aluminium deposition by cathodic pulverization on a wafer followed by AZ1518 resist spin coating (4,000 rpm, 8 s), a pre-baking during 60 s at 110°C, exposure to UV light through a chromium-glass mask and post-baking. The resist is revealed in a AZ726 remover bath. The Al layer is locally etched by orthophosphoric acid and final silicium drilling is achieved by deep ICP-RIE etching using SF_6/O_2 mixed gas (Bosch process). These shadowmasks are completely reusable.

Once the pattern is defined using one of the two methods described above, the channels (Process 1) or the
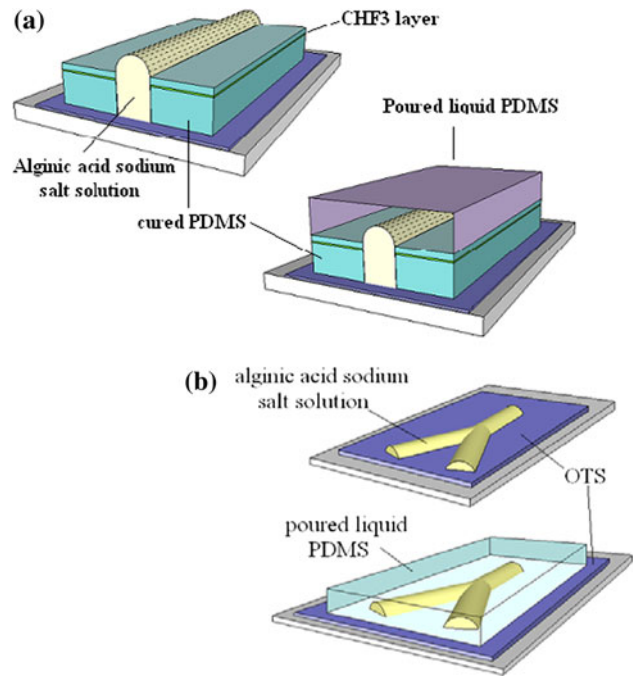

Fig. 6 a Semi-channel formation using the process I, **b** semi-channel formation using the process II

hydrophilic stripes (Process 2) are filled (Fig. 6a, b) with an aqueous solution of alginic acid sodium salt. Eventually, PDMS is then slowly poured on the rivulets, and dried at room temperature.

For channels with D as thickness of the 3D structuration layer and W as width, it must be mentioned that without the PDMS/CHF₃ stacks, the profile shown in Fig. 7 can be obtained, leading to an error of $[(2 \times D)/W] = 61\%$ on the roundness of the channel. With our method, only 10 μm of PDMS are left on each part of the channel, so the error at the end of the process never exceeds 5%.

The liquid deposition of alginate is realised manually using 30G syringes, using "drop by drop" deposition method. The aqueous solution is prepared by dissolving 6 g of alginic acid sodium salt powder in 300 mL of DI water leading to the following measured values: a density of 1.0072 g cm^{-3} and a kinematic viscosity of 1,630 cSt (or a dynamic viscosity of 1.642 Pa s).

When a semi-channel is obtained, it is then used to create a replica in two different ways: (a) cast again alginic acid sodium salt solution and recover with liquid PDMS,
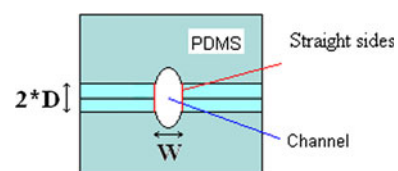

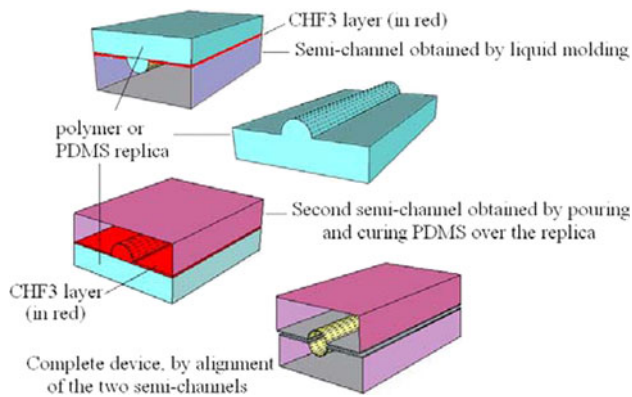**Fig. 7** Channel processed without the PDMS/CHF₃ stacking method

Fig. 8 Channel replication

(b) deposit CHF$_3$ as an anti-adhesive layer on the semi-channel and use PDMS or another more hard-wearing polymer to create a reusable negative mould.

Successive mouldings are performed at room temperature. If a residual film of dried alginic acid sodium salt is found on the cured PDMS, it is easily mechanically removed, but can also be dissolved using citrate aqueous solutions. It can also be let in place, and be used as bio-compatible coating.

At the end, the two parts are exposed to O$_2$ plasma, aligned under a microscope with help of methanol, and pressed together to form the channel.

Figure 8 schematically depicts the second technique:

3 Results and discussion

From the results reported in the literature, photolithography (Wang et al. 2007) provides very good results (70° TCA, 500 μm wide channels). Original techniques such as photocopying (Tan et al. 2001) or metal wire moulding (Song et al. 2010) give either low TCA (5°) or channels without junctions. In the present study, we propose to go further by experimentally analysing the links between the four main key parameters that we had identified in order to get large TCA values: (1) the choice of the liquid for the mould, (2) the aspect ratio between channel's height and width, (3) the value of the inner SCA, (4) the volume of the liquid deposited in the channel.

These analyses gave rise to two simple fabrication methods of closed round microchannels with various shapes and dimensions, with results at the state of art level.

Below we show two pictures of the straight channels obtained using process I. The channels produced have a length of 1.5 cm.

Figure 9 shows the channel before PDMS pouring onto the alginic sodium salt rivulet, while Fig. 10 illustrates the channel after the liquid moulding, but before the peeling of
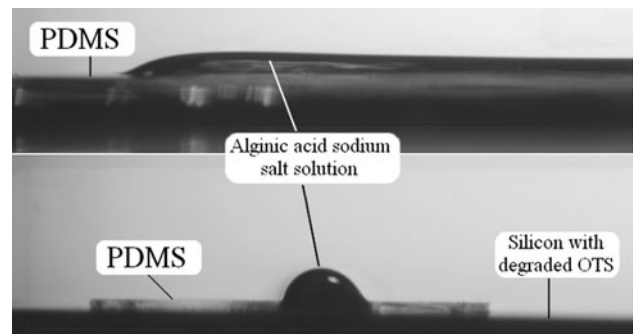

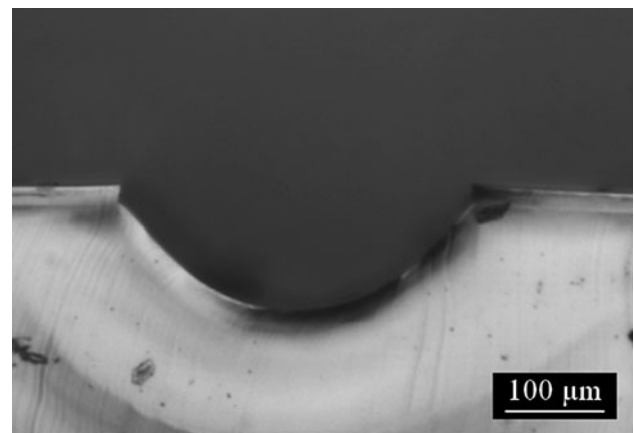Fig. 9 The meniscus shape of alginic acid sodium salt solution rivulet before PDMS pouring

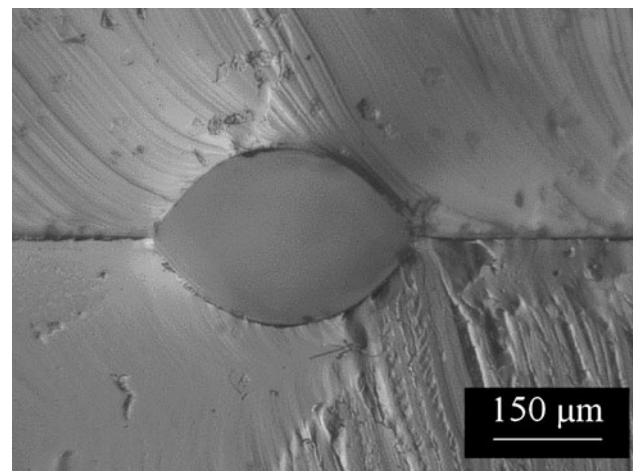Fig. 10 Front view of a 65° TCA, 350 μm wide straight half-channel

Fig. 11 Front view of a 75° TCA, 350 μm wide straight and closed channel

the straight sides. Figure 11 depicts a sealed channel with a TCA of 75°.

The second process based on OTS degradation through a shadowmask enables to vary more easily the shape of the

channels. Conditions on the volume deposited and inner angle values are the same as for the process I.

However, for the straight and Y-shaped channels, the control of the gradient between the "outer" and "inner" angles is more difficult due to the substrate and shadow-mask sensitivity to superimposition. Indeed, blurred patterns cannot be tolerated.

The results obtained with process II are then less impressive than those obtained with the process I, giving 55° as the best measure, and at the best, branches of 1 cm long. Figure 12 displays optical images of the same Y-shaped channel at various steps of fabrication: (a) image of a semi-channel, (b) channel sealed and filled with a blue ink.

3.1 Aspect ratio

Seemann et al. (2005) have demonstrated that rivulets shape and behavior depend on aspect ratio parameter between channels height and width. Their study consisted in a 3D structuring with the same SCA between the top and
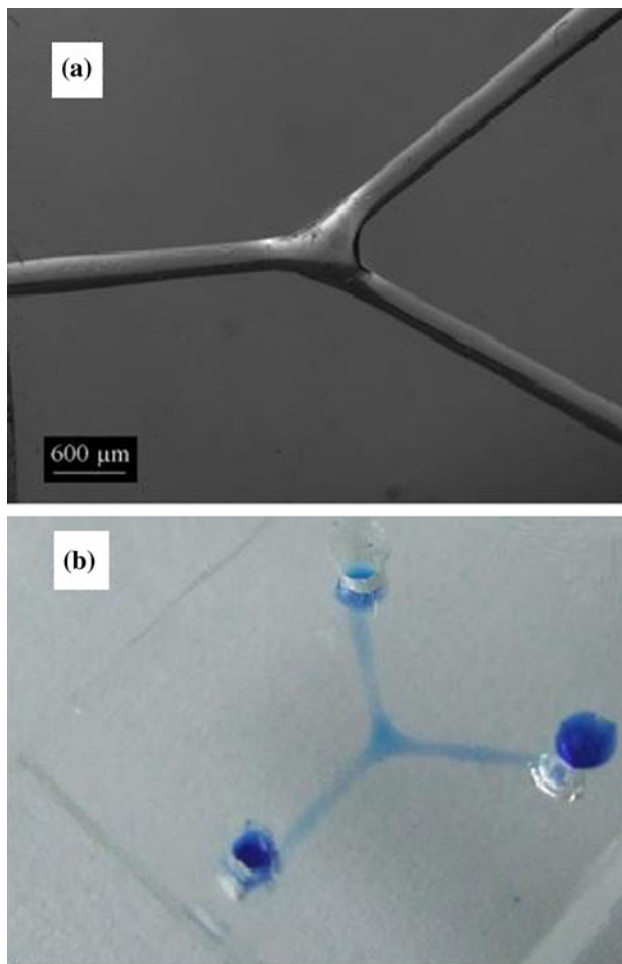

Fig. 12 Y-shaped 350 μm wide channel

bottom of a channel (same "inner" and "outer" angles). They have investigated theoretically the morphology of liquid rivulets as a function of the channel aspect ratio X (defined as depth on width, $X = D/W$) and SCA (which was varied from 5° to 80°), and obtained a diagram determining the behavioral zones (bulge, rivulet, concave meniscus) of liquid on the surface. This diagram was adapted for the present work to optimize the processes (see Sect. 3.2 below).

To create straight channels, PDMS stripes of approximately 140 μm in thickness were used, with the aim to fabricate 300 μm wide channels. These values led to an aspect ratio of $X = 140/300 = 0.46$ and a maximum TCA $\approx 82°$ has been measured after moulding. Important care has been devoted to preserve the PDMS flatness during the spin coating of the wafers and reporting of layers. Indeed, it has been observed that a deflection larger than 5% leads to process failure (see supporting information figure S1 for definition of the deflection notion).

3.2 Value of the inner contact angle

Concerning the value of the inner contact angle, the choice to use uniformly degraded OTS (80°) is dictated by the empirical law $\alpha_F = \theta + 90° = 180°$ reported by Seemann et al. (2005) to describe the "fattest" rivulet that can be obtained in their (F+) regime (liquid filaments without wedges). In this equality, the α_F corresponds to our TCA plus 90°, and θ corresponds to their uniform SCA. Then, the condition to get the "fattest" rivulet in their study is obviously to have SCA value $\theta = 90°$. However, our experimental tests revealed that the results are better if the angle chosen is slightly smaller than this limit. Thus we used degraded OTS layers with a SCA of 80°.

3.3 Relation between aspect ratio and inner contact angle

We have experimentally investigated the liquid rivulets formation for aspect ratios varying from 0.1 to 0.5 and inner angles from 30° to 90°. Figure 13 exhibits the measured TCA of the rivulets after the complete fabrication of a straight channel as a function of the inner angle and aspect ratio (the inner angle is known before alginic acid sodium salt solution deposition and the outer angle is always 110°). From this figure, we can deduce that:

1. for a high inner angle (>60°) and an aspect ratio higher than 0.15, the TCA values for the channels range from 65° to 75°, which corresponds to fairly round channels. Compared to the previous attempts with liquid moulds (Tan et al. 2001; Grimes et al. 2008; Chao et al. 2007; Liu et al. 2009), the performance here represents a step forward.
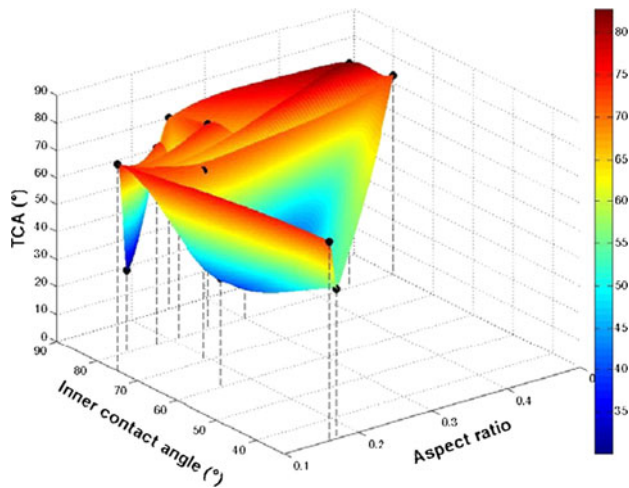
Fig. 13 Channel TCA as a function of the inner angle and aspect ratio of the channel (for more details see supporting information Table S2)

2. for an inner angle below 60° and/or an aspect ratio lower than 0.15 or higher than 0.5, the conditions are pretty unstable, and the channels have lower TCA values.

All the behaviors theoretically predicted by Seemann et al. (2005) for very small channels were experimentally identified, even if our channels are about 10 times bigger than theirs. However, the range of parameters of our curves by superimposition on their "phase diagram" is slightly different. It can be explained as the consequence of the main difference between our experimental conditions and the frame of their theory: we used different "outer" and "inner" angles between the top and bottom sides of the channels (as defined in Fig. 2) while they have the same value for both contact angles (no wetting contrast), and we used alginic acid sodium salt solution to create the rivulets while they used liquid structures created by vapour condensation of polystyrene.

3.4 Volume of liquid

Another important parameter is the volume of liquid deposited in the channels. Darhuber et al. (2000) showed that there is a link between the volume of liquid on the hydrophilic stripe and a "bulge" state. They have proposed an inequality (Eq. 1) to evaluate the maximum of volume to deposit, and demonstrated that the control of SCA contrast (between the "outer" and "inner" angles) is crucial to avoid the rivulet overflow. Here, V is the volume of liquid deposited on the pattern, l and w are, respectively, the length and the width of the pattern, and α is the rivulet TCA.

$$\frac{V}{l} < \frac{w^2}{4\sin^2\alpha}\left(\alpha - \frac{1}{2}\sin^2\alpha\right) \qquad (1)$$

In our case, the TCA of the liquid cylinder is controlled by the volume of the liquid deposited. The maximum volume is limited by the bulge formation, as demonstrated before (Gau et al. 1999; Lipowsky 2001; Lipowsky et al. 2005a, b).

Figure 14 exhibits a bulge, which appears in a microchannel if a large amount of liquid is deposited.

The maximum volumes which can be deposited into the channels, depending of their characteristics (width, length, SCA) have been measured and calculated using Eq. (1). The comparative results are given in Table 2.

We noticed that the volume of alginic acid sodium salt solution initially deposited is larger, approximately twice, than the volume predicted by Darhuber et al. (2000) as shown in Table 2. It can be explained by the differences between the methods and the experimental conditions employed.

To create straight channels with high TCA values, we took advantage of the bulge formation. The alginic acid sodium salt aqueous solution stripe is achieved by gently adding liquid until the bulge begins to form. Then, as the volume involved is small, evaporation occurs. A camera is used to visualize the bulge appearance and disappearance. Then the rivulet mould is covered with PDMS at the time corresponding to the disappearance of the bulge, when the rivulet becomes stable again.
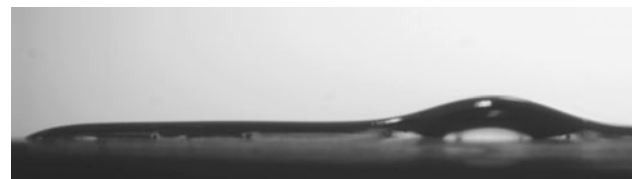

Fig. 14 Bulge formation in a microchannel

Table 2 Liquid volume's to deposit in the channels, according to Darhuber et al. formula, to avoid overflow

Channel width (μm)	Channel length (μm)	Theta (°) from Eq. (1)	Volume from Eq. (1) to deposit (μL)	Real volume deposited (μL)
200	5,000	55	0.036	0.08
		80	0.063	0.13
	10,000	55	0.073	0.17
		80	0.13	0.25
400	5,000	55	0.15	0.27
		80	0.25	0.50
	10,000	55	0.29	0.55
		80	0.5	0.90

4 Conclusion

We have optimized the morphology of a liquid rivulet at steps edges by controlling the wetting state. Circular microchannels ranging from 300 to 500 μm in diameter have been fabricated, with a TCA of 75° for straight channels and 55° for the Y-shaped ones. The processes proposed in this study offer several advantages: (1) they can be operated at ambient temperature, (2) they are adapted to tailor channels into soft and biocompatible materials like PDMS, (3) the processing onto various substrates (glass…) is possible, (4) they are achievable with simplicity, cheapness and rapidity (completed within a few hours), (5) quantitative results are at the state of the art, and (6) only basic equipments are required.

We believe that the technique reported in this work is useful for many microfluidic applications (their roundness reduce the fluid strengths of friction) such as cells separation/distribution.

References

Abbas A, Supiot P, Mille V, Guillochon D, Bocquet B (2009) Capillary microchannel fabrication using plasma polymerized TMDS for fluidic MEMS technology. J Micromech Microeng 19:045022

Abdelgawad M, Wu C, Chien WY, Geddie WR, Jewett MAS, Sun Y (2010) A fast and simple method to fabricate circular microchannels in polydimethylsiloxane (PDMS). Lab Chip 11:545–551

Brinkmann M, Blossey R (2004) Blobs, channels and "cigars": morphologies of liquids at a step. Eur Phys J E 14:79–89

Brinkmann M, Lipowsky R (2002) Wetting morphologies on substrates with striped surface domains. J Appl Phys 92:4296–4306

Chao SH, Carlson R, Meldrum DR (2007) Rapid fabrication of microchannels using microscale plasma activated templating (μPLAT) generated water molds. Lab Chip 7:641–643

Coffinier Y, Janel S, Addad A, Blossey R, Gengembre L, Payen E, Boukherroub R (2007) Preparation of superhydrophobic silicon oxide nanowire surfaces. Langmuir 23:1608–1611

Darhuber AA, Troian SM, Miller SM, Wagner S (2000) Morphology of liquid microstructures on chemically patterned surfaces. J Appl Phys 87:7768–7775

Futai N, Gu W, Takayama S (2004) Rapid prototyping of microstructures with bell-shaped cross-sections and its application to deformation-based microfluidic valves. Adv Funct Mater 16:1320–1323

Garra J, Long T, Currie J, Schneider T, White R, Paranjape M (2002) Dry etching of polydimethylsiloxane for microfluidic systems. J Vac Sci Technol A 20:975–982

Gau H, Herminghaus S, Lenz P, Lipowsky R (1999) Liquid morphologies on structured surfaces: from microchannels to microchips. Science 283:46–49

Grimes A, Breslauer DN, Long M, Pegan J, Lee LP, Khine M (2008) Shrinky dink microfluidics: rapid generation of deep and rounded channels. Lab on a Chip 8:170–172

Hongbin Y, Guangya Z, Siong CF, Shouhua W, Feiwen L (2009) Novel polydimethylsiloxane (PDMS) based microchannel fabrication method for lab-on-a-chip application. Sens Actuators B 137:754–761

Kang E, Shin SJ, Lee KH, Lee SH (2010) Novel PDMS cylindrical channels that generate coaxial flow, and application to fabrication of microfibers and particles. Lab Chip 10:1856–1861

Lee K, Kim C, Shin KS, Lee J, Ju BK, Kim TS, Lee SK, Kang JY (2007) Fabrication of round channels using the surface tension of PDMS and its application to a 3D serpentine mixer. J Micromech Microeng 17:1533–1541

Lenz P (1999) Wetting phenomena on structured surfaces. Adv Mater 11:1531–1534

Lipowsky R (2001) Structured surfaces and morphological wetting transitions. Interface Sci 9:105–115

Lipowsky R, Brinkmann M, Dimova R, Franke T, Kierfeld J, Zhang XZ (2005a) Droplets, bubbles, and vesicles at chemically structured surfaces. J Phys Condens Matter 17:S537–S558

Lipowsky R, Brinkmann M, Dimova R, Haluska C, Kierfeld J, Shillcock J (2005b) Wetting, budding, and fusion—morphological transitions of soft surfaces. J Phys Condens Matter 17:S2885–S2902

Liu X, Wang Q, Qin J, Lin B (2009) A facile "liquid-molding" method to fabricate PDMS microdevices with 3-dimensional channel topography. Lab Chip 9:1200–1205

Luo LW, Teo CY, Ong WL, Tang KC, Cheow LF, Yobas L (2007) Rapid prototyping of microfluidic systems using a laser-patterned tape. J Micromech Microeng 17:N107–N111

Mortensen NA, Okkels F, Bruus H (2005) Reexamination of Hagen-Poiseuille flow: shape dependence of the hydraulic resistance in microchannels. Phys Rev E 71:057301

Piriz AR, Cortazar OD, Cela JJL, Tahir NA (2006) The Rayleigh-Taylor instability. Am J Phys 74:1095–1098

Seemann R, Brinkmann M, Kramer EJ, Lange FF, Lipowsky R (2005) Wetting morphologies at microstructured surfaces. Proc Natl Acad Sci 102:1848–1852

Song SH, Lee CK, Kim TJ, Shin IC, Jun SC, Jung HI (2010) A rapid and simple fabrication method for 3-dimensional circular microfluidic channel using metal wire removal process. Microfluid Nanofluid 9:533–540

Speth RL, Lauga E (2009) Capillary instability on a hydrophilic stripe. New J Phys 11:075024

Tan AM, Rodgers K, Murrihy JP, O'Mathuna C, Glennon JD (2001) Rapid fabrication of microfluidic devices in poly(dimethylsiloxane) by photocopying. Lab Chip 1:7–9

Wang GJ, Ho KH, Hsu SH, Wang KP (2007) Microvessel scaffold with circular microchannels by photoresist melting. Biomed Microdevices 9:657–663

West J, Michels A, Kittel S, Jacob P, Franzke J (2007) Microplasma writing for surface-directed millifluidics. Lab Chip 7:981–983